Exploiting Scaling Laws for Designing Polymeric Bottle Brushes: a Theoretical Coarse Graining for Homopolymeric Branched Polymers

Pietro Corsi,[1] Elia Roma,[1] Tecla Gasperi,[1] Fabio Bruni,[1] and Barbara Capone[1,*]

[1]*Dipartimento di Scienze, Università degli Studi Roma Tre, Via della Vasca Navale 84, 00146, Roma, Italy*

(Dated: May 28, 2022)

Bottle brushes are polymeric macromolecules made of a linear polymeric backbone grafted with side chains. The choice of the grafting density σ_g, of the length n_s of the grafted side chains and their chemical nature, fully determines the properties of each macromolecule, such as its elasticity and its folding behaviour. Typically experimental bottle brushes are systems made of tens of thousands of monomeric units, rendering a computational approach extremely expensive, especially in the case of bottle brushes solutions. A proper coarse graining description of these macromolecules, thus appears essential. We here present a theoretical approach able to develop a general, transferable and analytical multi-scale coarse graining of homopolymeric bottle brush polymers under good solvent condition. Starting from scaling theories, each macromolecule is mapped onto a chain of tethered star polymers, whose effective potential is known from scaling predictions, computational and experimental validations and can be expressed as a function of the number of arms f, and on the length n_a of each arm. Stars are then tethered to one another and the effective potentials between them is shown to only depend on the key parameters of the original bottle brush polymer (σ_g, n_s). The generalised form of the effective potential is then used to reproduce properties of the macromolecules obtained both with scaling theories and with simulations. The general form of the effective potentials derived in the current study, allows to describe theoretically and computationally properties of homopolymeric bottle brush polymers for all grafting densities and all lengths of both backbone and grafted arms, opening the path for a manifold of applications.

PACS numbers: 82.70.-y, 81.16.Fg, 05.10.-a, 83.80.Uv

INTRODUCTION

Scaling theories are a powerful tool allowing to map properties of extremely complex systems onto simple relations linking a selection of microscopic details to a subset of general features. Polymers, due to their fractal nature, are an excellent example of systems that can extensively be described by means of scaling theories for the most diversified architectures and chemical compositions [1]. The average size (or radius of gyration R_g) of a single polymeric macromolecule can be, for example, mapped onto a power law linking the number of monomers n to a critical exponent ν that grasps the monomer-solvent interaction [2]: $R_g \sim n^{\nu}$. Scaling laws also apply to finite density systems either made of free macromolecules in solution or characterised by complex geometrical constraints. In this context, general properties of polymeric brushes can be described by means of simple scaling considerations [1, 3, 4] as well as through mean-field self-consistent calculations [5–7]. For polymeric systems grafted on a planar surface, scaling predictions allow to estimate the dependence of average height of a brush in terms of the grafting density $\sigma_g = N/A$ - expressed as the average number N of polymers grafted per unit area A - the length n of the grafted polymers, and of the interaction between the monomers and solvent [1, 3]:

$$h \sim n\sigma_g^{\frac{1-\nu}{2\nu}}. \tag{1}$$

The results obtained for the planar case can then be generalised to brushes with spherical symmetry [8], that find their macromolecular correspondent in star-like polymers [9–11]. Similarly to how the average height of a planar brush was computed, it is possible to estimate the scaling law of the average radius of gyration of such macromolecules in terms of the number n_a of monomers belonging to each of the f arms grafted on a central core :

$$R_s \sim n_a^{\nu} f^{1/5}, \tag{2}$$

where for simplicity we assume the radius of gyration of the star to scale with the $1/5$ exponent [8], neglecting finite size corrections to the scaling exponent linked to anisotropy that can arise in stars with a small number of arms.

Further works extended the theories of planar and spherical brushes to different geometries and to more complex grafting units [12, 14, 15]. The present manuscript focuses on the properties of the so-called bottle brush polymers, i.e. macromolecules made of a polymeric backbone of n_b monomers, grafted with linear chains each one made of n_s monomeric units. The grafting density is expressed as $\sigma_g = 1/(bm)$, where bm is the unit of length between each grafting site expressed as the product of the number of m monomers between the diverse grafting sites, and the equilibrium distance b between bonded neighbouring monomers. In the following part of this work b is set to one, and all the simulations performed in good solvent condition, hence $\nu \sim 0.588$.

As side-chains fluctuate, the average monomer distribution around the backbone and the average height of the grafted homopolymeric chains can be predicted by assuming a tubular conformation for the macromolecule [16, 17].

The tube diameter D_c has been shown to scale as [12]:

$$D_c = 2R_c \sim n_s^{\nu}\tau^{1/5}\left(\sigma_g n_s\right)^{\nu/5}, \tag{3}$$

where the solvent quality is taken into account both in the Flory exponent ν and the reduced temperature $\tau = (T-\theta)/T$,

where T is the temperature of the system and θ is the θ-temperature e.g. the transition temperature between good solvent and bad solvent, at which polymers behave as random walks. As we do not change nor the temperature nor the solvent quality throughout this work, τ is constant. By neglecting all contributions arising from constant terms, we obtain the following scaling law for the cylinder diameter: $D_c \sim n_s^{\nu} (\sigma_g n_s)^{\nu/5}$.

The radius of gyration R_{bb} of the whole macromolecule can be written as [12]:

$$R_{bb} \sim N^{\nu} \tau^{1/5} (\sigma_g n_s)^{-2\nu/5} \sim n_b^{\nu} (1+\sigma_g n_s)^{\nu} (\sigma_g n_s)^{-2\nu/5}, \quad (4)$$

where in the last term we ignore all constant terms, and write explicitly the total number of monomers $N = n_b(1+\sigma_g n_s)$.

The large number of microscopic units constituting each bottle-brush renders an extensive computational study of these macromolecules prohibitive from a computational point of view. On the other hand, despite the progresses obtained in describing the system by means of scaling laws, detailed analyses either at finite density, or when particular phenomena have to be investigated, are still difficult to access. An effective description invokes a reduction of the degrees of freedom to be analysed, making of paramount importance the development of an efficient and quantitative multi-scale strategy.

This work is structured in two distinct sub-sequent sections; we first use full monomer Molecular Dynamics (MD) simulations to extract the key information and the set of effective potentials that we will need to perform the proposed coarse graining (CG). We then use the newly derived potentials to reproduce and compare the results obtained with CG to the full monomeric MD results, and to scaling predictions.

RESULTS AND DISCUSSION

The full monomer representation: deriving scaling laws and effective potentials

All calculations, both in the full monomer case as well as for the coarse grained representation, are done by means of MD simulations, performed with LAMMPS [19] in the NVT ensemble. In the full monomer representation, monomers in the simulations interact through a purely repulsive truncated and shifted Lennard-Jones potential (i.e, good solvent conditions),

$$V_{LJ}(r) = \begin{cases} 4\varepsilon \left[\left(\frac{\sigma}{r}\right)^{12} - \left(\frac{\sigma}{r}\right)^{6} \right] + \varepsilon & \text{for } r \leq 2^{1/6}\sigma \\ 0 & \text{for } r > 2^{1/6}\sigma \end{cases} \quad (5)$$

with a cutoff set at $2^{1/6}\sigma$.

Bonded monomers are tethered by means of a Finite Extensible Nonlinear Elastic (FENE) potential [13]:

$$V_{\text{FENE}}(r) = -0.5kR_0^2 \ln\left[1-\left(\frac{r}{R_0}\right)^2\right] + 4\varepsilon\left[\left(\frac{\sigma}{r}\right)^{12} - \left(\frac{\sigma}{r}\right)^{6}\right] + \varepsilon \quad (6)$$

where $k = 30\varepsilon/\sigma^2$ and $R_0 = 1.5\sigma$.

In the following part of this work, we use the reduced parameters T (temperature), ε (interaction energy), and $\sigma = 1$ (monomer diameter) .

The full monomeric simulations have been performed on bottle brushes made of a backbone of $n_b = 300$ monomers, with side chains of n_s monomers in the range $n_s \in [50, 300]$ for the various analysed cases, with an increment of $\delta n_s = 25$ monomers between one case and another, and grafting densities $\sigma_g = 0.2, 0.25, 0.33, 0.5$.

Simulations are performed on macromolecules made of a total number of monomers in the $10^3 - 10^5$ range for at least 10^8 MD steps.

We first compute, within the full monomeric representation, general properties of the single bottle brush, such as the average cylinder radius R_c and the average radius of gyration R_{bb} for a wide set of (σ_g, n_s) combinations, as shown in Figure 1 (a) and (b).

R_c can be extrapolated as the average distance of all monomers belonging to the grafted arms from the backbone. The probability distribution $P(r_\perp)$ of the monomer height, computed as the distance of all monomers along the orthogonal direction to the backbone, is shown in panel (c) of Figure 1. By rescaling the $P(r_\perp)$ computed for all of the (σ_g, n_s) combinations, with the corresponding cylinder radius $R_c(\sigma_g, n_s)$, we obtain the perfect rescaling of all curves onto a general mastercurve.

Early works on scaling behaviours of bottle brush polymers, [14, 15, 18] suggested that the length of the rigid portion of a bottle brush macromolecule is of the order of its cylinder diameter, or thickness. This renders possible to define within each macromolecule spherical symmetric elements - or *super blobs* - characterised by having a constant rigidity on a scale of the order of the cylinder diameter D_c. This work aims at developing a consistent and general coarse grained representation for homopolymeric bottle brushes in good solvent condition. The idea that will be exploited, is that each macromolecule can be seen as a chain of star-like *super blobs*, hence the coarse graining procedure will require three major steps:

1. identification of the number ξ of super blobs that will be used to represent the macromolecule;
2. mapping of each super blob onto an equivalent star polymer;
3. derivation of a general form for the set of effective potentials acting between the coarse grained beads.

We sketch the coarse graining scheme in Figure 2; panel (a) highlights the division of the bottle brush into super blobs of radius R_ξ, while panel (b) shows the mapping of each super

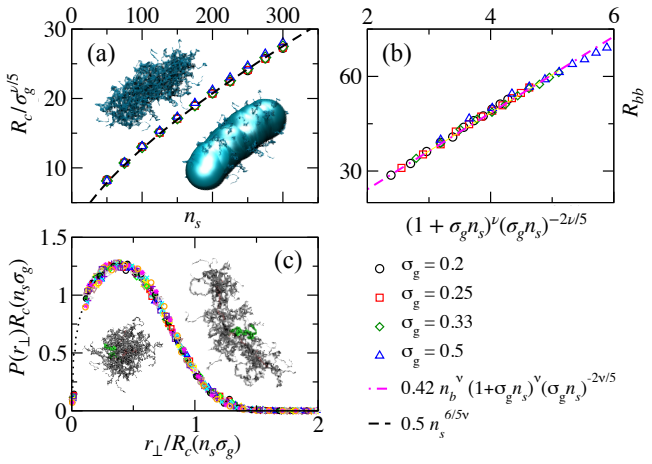

Figure 1: All plots are obtained for bottle-brushes made of $n_b = 300$ monomers per backbone, with grafting densities $\sigma_g = 0.2, 0.25, 0.33$ and 0.5 and arms of length $n_s \in [50, 300]$ with $\delta n_s = 25$ monomers per chain. Top left panels shows scaling laws for R_c as in (3), top right shows the scaling of the radius of gyration R_{bb} as in (4) and the bottom left panel shows the distribution $P(r_\perp)$ of monomers around the backbone, rescaled with the scaling law in equation (3). Snapshots in the top left panel show a bottle brush made by a backbone of $n_b = 300$, with grafting density $\sigma_g = 0.5$ and arms made of $n_s = 300$ monomers, and the same brush enclosed in a cylinder of radius $R_c(\sigma_g = 0.5, n_s = 300)$. The snapshots in the bottom left figure highlight - in green - one of the arms of a bottle brush made of $n_b = 300$ backbone monomers, with grafting density $\sigma_g = 0.2$ and arms made of $n_s = 125$ monomers. Side and top view show the way in which arms distribute around the backbone

blob into a star polymer of radius $R_s = R_\xi$ made of a number f_{eq} of arms each one with $n_a = n_s$ monomers.

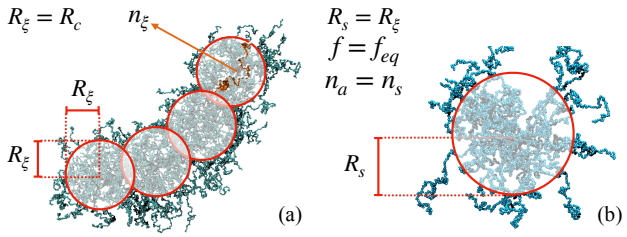

Figure 2: Schematic representation of the coarse graining procedure. Panel (a) sketches the super blobbing of the bottle brush macromolecules into ξ spheric-symmetrical blobs. Each blob contains a number n_ξ of backbone monomers as defined in equation (7) and higlighted in red. Panel (b) is a zoom on one of the ξ super blobs that will become basic units of the coarse grained representations. Each super blob is represented as a star polymer of radius $R_s = R_\xi$, made of $f = f_{eq}$ arm of $n_a = n_s$ monomers. Blobs interact with one each other by means of the effective star-star potential (9).

1. Counting the number of super blobs

To identify the number of blobs, we exploit the spherical symmetry that each bottle brush presents on sub-portions of the macromolecule of lengths comparable to the cylinder radius. We therefore divide the brush in a number ξ of identical sub-bottle brush segments, each one made of n_ξ backbone monomers, such that the radius of gyration R_ξ of the segment is identical to the radius of the cylinder.

By imposing $R_\xi = R_c$ in (4) we obtain the number of n_ξ of backbone monomers belonging to each of the of the ξ subsegments of the bottle brush

$$n_\xi \sim \frac{R_c^{1/\nu}}{(1+\sigma_g n_s)(\sigma_g n_s)^{-2/5}}. \tag{7}$$

The number $\xi = n_b/n_\xi$ of super blobs per bottle brush is then obtained as the integer ratio between the number of monomers per backbone and the number of monomers per blob.

2. Identify the equivalent star

We now want to identify the equivalent star on which we will map each super blob. In particular we want to derive the number f_{eq} of equivalent arms, made of n_s monomers each, needed so that the radius of gyration of the equivalent star polymer is identical to the radius of gyration of a bottle brush made of n_ξ backbone monomers, with arms of n_s monomers and a grafting density σ_g.

Equating (2) and (3) we obtain $R_s = R_\xi = R_c$. It can be easily derived that the equivalent star has a number of arms:

$$f_{\rm eq} \sim (R_c/n_s^{\nu})^5 \sim \left[\left(n_s^{\nu}(\sigma_g n_s)^{\nu/5}\right)/n_s^{\nu}\right]^5 \sim (\sigma_g n_s)^{\nu} \tag{8}$$

each made of n_s monomers, as sketched in Figure 2.

3. Deriving the effective potential

The first step into the proposed coarse graining procedure is to assume that each super blob interacts with other super blobs by means of a star-like effective pair potential V_s [10, 20]:

$$\frac{V_s(r)}{k_B T} = \begin{cases} \frac{5}{18} f_{\rm eq}^{3/2}\left[-\ln\left(\frac{r}{\sigma_c}\right) + \left(1+\frac{\sqrt{f_{\rm eq}}}{2}\right)^{-1}\right] & \text{for } r \le \sigma_c \\ \frac{5}{18} f_{\rm eq}^{3/2}\left(1+\frac{\sqrt{f_{\rm eq}}}{2}\right)^{-1}\left(\frac{\sigma_c}{r}\right)\cdot & \\ \cdot\exp\left[-\sqrt{f_{\rm eq}}\left(\frac{r-\sigma_c}{2\sigma_c}\right)\right] & \text{for } r > \sigma_c \end{cases} \tag{9}$$

where $\sigma_c = (4/3)R_s = (4/3)R_c$ is the corona diameter of the star polymer.

To estimate the tethering potential linking neighbouring coarse grained beads, we compute the distribution of distances $P(r^i_{cm} - r^{i+1}_{cm})$ between the centres of masses of the neighbouring super blobs, e.g. between the centres of masses of consecutive sub-parts of the bottle brush made of n_ξ backbone beads. The logarithmic inversion of the probability distribution leads to the total potential acting between two neighbouring beads. Such an interaction will be modelled as the superposition of a repulsive potential and a tethering term $\Phi_{\rm th}(r)$:

$$V_\xi(r) = V_s(r) + \Phi_{\rm th}(r), \tag{10}$$

where $V_s(r)$ is the effective potential between two equivalent stars as in equation (9), and $\Phi_{\rm th}$ a tethering term that has the form:

$$\Phi_{\rm th}(r) = k(r - r_0)^2, \tag{11}$$

where $k = 5/18\sigma_g^2 n_s$ and $r_0 = \sigma_c$.

The k and r_0 values have been determined by analysing all of the (σ_g, n_s) combinations that we defined earlier on in this section. For clarity we show in panel (a) of Figure 3 only one amongst the possible sets of effective potentials that can be obtained for all the (σ_g, n_s) combinations; in particular we present the potentials that are used to map a bottle brush with $\sigma_g = 0.5$ and $n_s = 300$ onto a chain of stars of $f_{\rm eq} = 19$ equivalent arms. The inset shows the comparison between the theoretical predictions for the total potential acting between two tethered beads, and the raw data obtained by logarithmically inverting the probability distributions for four (σ_g, n_s) combinations as specified in the caption. Panel (b) of Figure 3 shows the fitting result for the elastic constant k obtained with all of the extracted potentials.

Remarkably, the set of effective potentials obtained in (10) only depend on a few details of the microscopic system, and can be described through a functional form. The sets of effective interactions obtained are thus general: all systems with the most diverse microscopic characteristics can be reproduced by the set of potentials just introduced, where (9) is the potential acting between non bonded units, while bonded units interact via the effective potential in (10).

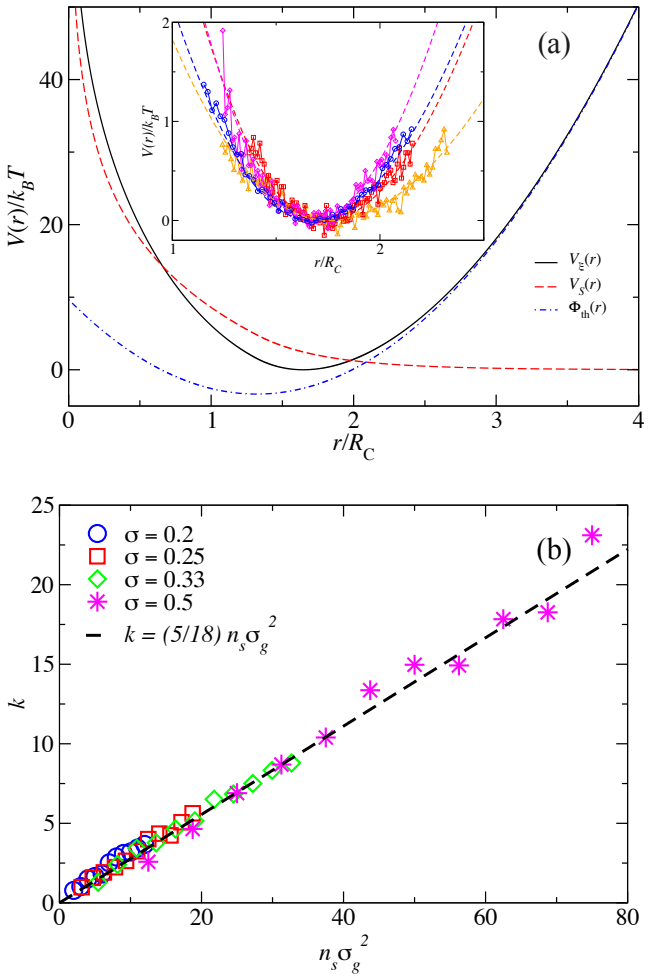

Figure 3: Panel (a): the effective potential acting between two neighbouring super blobs (black solid curve) split into the equivalent star polymer contribution (red dashed curve) and the tethering therm $\Phi_{\rm th}(r)$ (blue dash-dotted curve). The inset of the figure shows raw data vs theoretical fitting of the total tethering potentials between neighbouring subparts of the bottle brushes for $\sigma_g = 0.2, n_s = 100$, (orange), $\sigma_g = 0.25, n_s = 150$ (red), $\sigma_g = 0.33, n_s = 125$ (magenta), $\sigma_g = 0.5, n_s = 50$ (blue) Panel (b) shows the fitting of all of the spring constants k leading to the theoretical form in equation (11).

Testing the coarse graining procedure: bottle brushes as linear homopolymeric chains made of tethered star polymers

To test the coarse graining procedure, we performed a series of computational analyses by representing classes of generality of bottle brushes as linear homopolymeric chains. The monomeric units of each coarse grained molecule are coarse-grained star polymers, that interact with one each other by means of the purely repulsive potential (9), and are tethered by means of the effective interaction (11).

The mapping between the underlying full monomer representation and the coarse grained one, lies in the choice of the microscopic parameters (σ_g, n_s) that univocally determine the bottle brush cylinder radius R_c. The latter becomes the unit length for the monomeric beads of the coarse grained chain $R_s = R_c = R_\xi$. This reflects on the f_{eq} value, thus on the particular set of effective interactions to be used between all super blobs. As for the mapping of the backbone length, since the number n_ξ of backbone monomers per blob is fixed by the choice of R_c in (7), a variation of the number ξ of super blobs implies a change in the total microscopic backbone monomers per molecule $n_b = \xi n_\xi$. The more the blobs used, the longer the corresponding backbone.

We performed MD simulations, and computed the radius of gyration for coarse grained homopolymeric chains made of $\xi = 5, 10, 15, 20, 25, 30, 50, 100, 200$ effective monomers, for systems that correspond - on the microscopic level - to all

of the combinations of $\sigma_g = 0.2, 0.25, 0.33, 0.5, 1$ and $n_s = 50, 100, 200, 400, 600, 800$.

To check the consistency between the two representations, we compute the radius of gyration for all of the aforementioned systems in the coarse grained representation and map it to the monomer resolved bottle brush one (4). To perform the mapping, the first step is to compute from the ξ coarse grained beads the underlying monomer resolved number of backbone monomers:

$$n_b = \xi n_\xi \sim \xi \frac{R_c^{1/\nu}}{(1+\sigma_g n_s)(\sigma_g n_s)^{-2/5}}. \qquad (12)$$

The radius of gyration of linear homopolymeric chain made of n beads of radius R_c is know to scale as [2]

$$R_g \sim R_c n^\nu. \qquad (13)$$

To compare the radii of gyration obtained with the two models, we thus need to compare (13) and (4) for all of the measured systems:

$$R_{bb} \sim n_b^\nu (1+\sigma_g n_s)^\nu (\sigma_g n_s)^{-2\nu/5} \sim R_g. \qquad (14)$$

We thus obtain a general relation between the two representations:

$$R_g/(1+\sigma_g n_s)^\nu (\sigma_g n_s)^{-2\nu/5} \sim n_b^\nu, \qquad (15)$$

where R_g in the left hand of equation (15) is computed in the coarse grained representation.

We show in Figure 4 all of the data obtained with the here introduced coarse grained method, falling on the predicted mastercurve (15), together with a line highlighting the correct dependence of $R_g/(1-\sigma n_s)^\nu(\sigma n_s)^{-2\nu/5}$ on n_b. Three shapshots are also drawn: the top one shows a full monomer represented bottle brush, the middle coloured one is the full monomeric mapping - in terms of star polymers - corresponding to the original bottle brush, and the bottom one emphasises how each star is represented by means of its isotropic effective potential, shown as a sphere. The perfect agreement between all of the simulated systems, demonstrates the effectiveness of the coarse graining process. To assess the predictive power of the procedure, we extended simulations to the $\sigma_g = 1$ grafting density case, that had not been included in the derivation of the effective potential, reaching a reasonable agreement even for such a stiff molecule.

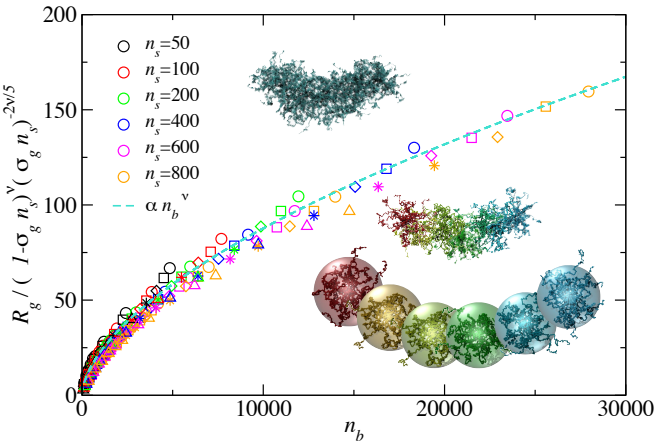

Figure 4: The plot shows the radius of gyration obtained by means of a coarse grained representation for the underlying bottle brush. The quantities reported on the y-axis has been rescaled according to equation (4), while the quantity plotted on x-axis has been rescaled using equation (12) to map results obtained by means of a homopolymeric representation on the predictions obtained with the scaling law of equation (4). Circles correspond to a microscopic grafting density of $\sigma_g = 0.2$, squares are $\sigma_g = 0.25$, diamond are $\sigma_g = 0.33$, stars are $\sigma_g = 0.5$, triangles are $\sigma_g = 1$, while the corresponding n_s are colour coded in the legend of the graph (black for n_s=50, red for 100, green for 200, blue for 400, magenta for 600 and orange for 800. The two snapshots show a bottle brush with $n_b = 300, \sigma_g = 1$ and $n_s = 225$ and the full monomeric view of a bottle brush made of a series of star polymers. α is a fitting constant.

CONCLUSIONS

Summarising, we introduced an accurate and extremely simple coarse grained methodology for homopolymeric bottle brushes based on scaling arguments. We derived a set of general effective potentials that can be used to represent the complex macromolecular systems as well as their functional dependence on a few microscopic details, and lay the basis for a further exploration of physical properties featured in complex macromolecules in diversified environments. We show that, within our coarse graining framework, macromolecules made of tens of thousands of monomers can be mapped onto a chain of a few effective beads, retaining the link between the coarse grained representation and the underlying microscopic one in the functional form of the effective potentials used. We tested the multiscale methodology by reproducing properties of the full monomeric molecules by means of our novel coarse grained representation. Notwithstanding the coarse grained molecules do not even retain the geometry of the original macromolecules, the results obtained with the multiscale approach have a *quantitative* agreement with both the full monomeric computational results, and with the predictions obtained with scaling laws, as shown in Figure 4. We in fact show that it is possible to map a full monomeric system characterised by a cylindrical geometry into a chain of spherical effective beads. The successful achievement of our quantitative coarse graining makes possible to access prohibitive regions, such as finite density analyses, that the large number of monomeric units involved would not allow to investigate with an monomeric description (each macromolecule is made of $\sim 10^3 - 10^5$ monomers). Consequently, the initial theoretical prediction of all interactions between the titled

macromolecule and its environment should give a facile access to the design and synthesis of bottle brushes suitable for a plethora of widespread uses. For example, the opportunity of foreseeing how to selectively tune the key interactions between each homopolymer and various bioactive compounds by simply changing either pH or temperature [21, 22], makes bottle brushes an extremely effective and efficient tool in the field of innovative drug delivery systems [23].

On a different perspective, the possibility of controlling the elastic properties of the macromolecules by tuning the (σ_g, n_s) combination, also renders finite density solutions of bottle brushes of extreme interest due to their peculiar rheological properties [24].

The present methodology will allow for numerous applications. It can, for instance, be easily generalised to cases of polydisperse bottle brushes, where a different local grafting density σ_g and/or a different local length n_s of the grafted arms will lead to a change in the elastic properties of the macromolecule. The coarse graining will allow to map such a case onto a chain of stars characterised by different radii of gyration, each represented by its corresponding effective potential, following the generalisation of the effective potential, as shown for example in reference [25]. The possibility to use this coarse graining representation to study the adsorbption properties of the bottle brushes, and to compare them to those of star polymer [11] is currently being investigated by the authors of this paper. Additionally, in order to experimentally validate our theoretical findings, the syntheses of various star polymers, as well as the corresponding bottle brushes, are ongoing in our laboratories and will be reported in due course.

ACKNOWLEDGMENTS

BC acknowledges funding from the Marie Curie Individual Fellowship, project ID 751255. ER acknowledge the financial support from Erasmus+ Unipharma Graduates 2017/2018 and the hospitality of University of Natural Resources and Life Sciences Vienna. The Grant of Excellence Departments, MIUR-Italy (ARTICOLO 1, COMMI 314 - 337 LEGGE 232/2016) is gratefully acknowledged.

* Electronic address: barbara.capone@uniroma3.it

[1] P. G. de Gennes, *Scaling Concepts in Polymer Physics* (Cornell University Press, 1980).
[2] P. Flory, *Principles of Polymer Chemistry* (Cornell University Press, 1953).
[3] S. Alexander, J. Phys. France **38**, 983 (1977).
[4] I. Coluzza, B. Capone, and J.-P. Hansen, Soft Matter **7**, 5255 (2011).
[5] S. T. Milner, T. A. Witten, and M. E. Cates, Macromolecules **21**, 2610 (1988).
[6] C. M. Wijmans, J. M. H. M. Scheutjens, and Y. B. Zhulina, Macromolecules **25**, 2657 (1992).
[7] R. R. Netz and M. Schick, Macromolecules **31**, 5105 (1998).
[8] M. Daoud and J. P. Cotton, J. Phys. France **43**, 531 (1982).
[9] M. Watzlawek, C. N. Likos, and H. Löwen, Phys. Rev. Lett. **82**, 5289 (1999).
[10] C. N. Likos, H. Löwen, M. Watzlawek, B. Abbas, O. Jucknischke, J. Allgaier, and D. Richter, Phys. Rev. Lett. **80**, 4450 (1998).
[11] D. Marzi, C. N. Likos, and B. Capone, The Journal of Chemical Physics **137**, 014902 (2012).
[12] T. M. Birshtein, O. V. Borisov, Y. B. Zhulina, A. R. Khokhlov, and T. A. Yurasova, Polymer Science U.S.S.R. **29**, 1293 (1987), ISSN 0032-3950.
[13] K. Kremer, G. S. Grest, J Chem. Phys. **94**, 4103 (1990)
[14] Y. B. Zhulina, Polymer Science U.S.S.R. **26**, 885 (1984), ISSN 0032-3950.
[15] Y. B. Zhulina and T. M. Birshtein, Polymer Science U.S.S.R. **27**, 570 (1985), ISSN 0032-3950.
[16] H.-P. Hsu, W. Paul, and K. Binder, Macromolecular Theory and Simulations **20**, 510 (2011).
[17] H.-P. Hsu, W. Paul, and K. Binder, Polymer Science Series C **55**, 39 (2013), ISSN 1555-614X.
[18] H.-P. Hsu, W. Paul, and K. Binder, Europhysics Letters **92**, 28003 (2010).
[19] S. Plimpton, Journal of Computational Physics **117**, 1 (1995), ISSN 0021-9991.
[20] C. N. Likos, Physics Reports **348**, 267 (2001), ISSN 0370-1573.
[21] X.-Y. Tu, C. Meng, X.-L. Zhang, M.-G. Jin, X.-S. Zhang, X.-Z. Zhao, Y.-F. Wang, L.-W. Ma, B.-Y. Wang, M.-Z. Liu, et al., Macromolecular Bioscience **18**, 1800022 (2018).
[22] X.-Y. Tu, C. Meng, Y.-F. Wang, L.-W. Ma, B.-Y. Wang, J.-L. He, P.-H. Ni, X.-L. Ji, M.-Z. Liu, and H. Wei, Macromolecular Rapid Communications **39**, 1870014 (2018).
[23] R. Verduzco, X. Li, S. L. Pesek, and G. E. Stein, Chem. Soc. Rev. **44**, 2405 (2015).
[24] W. F. M. Daniel, J. Burdynska, M. Vatankhah-Varnoosfaderani, K. Matyjaszewski, J. Paturej, M. Rubinstein, A. V. Dobrynin, and S. S. Sheiko, Nature Materials **15**, 183 (2016).
[25] C. Mayer, F. Sciortino, C. N. Likos, P. Tartaglia, H. Löwen, and E. Zaccarelli, Macromolecules **42**, 423 (2009).